POTENTIAL OF INVASIVE SHRUBS FOR ENERGY APPLICATIONS IN UGANDA

Fildah Ayaa[1*], Michael Lubwama[2], John Baptist Kirabira[2], Xi Jiang[3]

[1]Department of Agricultural and Bio-systems Engineering, Makerere University, P.O. Box 7062, **Kampala**, Uganda
[2]Department of Mechanical Engineering, Makerere University, P.O. Box 7062, **Kampala**, Uganda
[3]School of Engineering and Materials Science, Queen Mary University of London, Mile End Road, **London** E1 4NS, UK,

Corresponding Author Email: fildayaa@gmail.com

ORCID Identifiers: Fildah Ayaa 0000-0002-6850-5924
Michael Lubwama 0000-0001-7984-262X
John Baptist Kirabira 0000-0001-5047-1351
Xi Jiang 0000-0003-2408-8812

Abstract

In this study, six fast growing invasive biomass species; *Acacia mearnsii, Broussonetia papyrifera, Lantana camara, Mimosa pigra, Psidium guajava and Senna spectabilis* were studied to determine their potential for fuel and biofuel production. Proximate composition, ultimate composition and heating values were determined using standard methods. The thermal analysis, chemical interactions, and morphology were studied using Thermal Gravimetric Analysis (*TGA*), Fourier-Transform Infrared Spectroscopy *(FT-IR)*, and Scanning Electron Microscopy (*SEM)* analysis respectively. Aspen Plus Version 11 was used to simulate slow, fast and flash pyrolysis of the biomass. *Senna spectabilis* had the highest heating value of 17.84 MJ/kg and the lowest ash content, making it the most suitable for thermochemical conversion. Based on the compositional analysis, *Senna spectabilis* also had the highest content of cellulose (48 %), making it most suitable for biofuel production via enzyme saccharification. The Aspen Plus model for the pyrolysis process was used to predict the yields and products of pyrolysis of the biomass species for typical reactor conditions and feedstock composition. The highest yield of biogas, biochar and bio-oil were achieved at 650 °C for all the biomass species. Moreover, *Lantana camara* was the most suitable for biogas production and *Senna spectabilis* for biochar and bio-oil production. The influence of the pyrolysis temperature on the pyrolysis products, flue gases and gaseous emissions were also demonstrated in this study.

Keywords: *Biomass, Renewable Energy, Invasive shrubs*, *Pyrolysis, Modeling*

Article Highlights

- Invasive species are potential sources of biomass raw materials for bioenergy conversion processes
- Physicochemical properties of invasive biomass similar to published woody species and agricultural residues
- Upto 71-93 % biogas yield can be produced from the investigated biomass species at 800 °C

1 Introduction

A third of the world's population, nearly 2.5 billion people, cook with biomass (IEA, 2019). There are 754 million people in Africa who rely primarily on biomass for cooking energy, and 99 % of them live in Sub-Saharan Africa (SSA) (IEA, 2016B). Based on projections, the number of people who depend on traditional biomass in SSA will increase by 10 % by 2030, as the rate of electricity connections will not keep pace with population growth (Chirambo, 2016). In Uganda, approximately 96 % of households use wood fuels (wood and charcoal) as a major source of energy for cooking (Ministry of energy and mineral development, 2015; UBOS, 2014). However, the use of biomass for energy has been proven to be harmful to the environment and human health. The unsustainable harvesting of biomass fuels contributes to climate change and local forest degradation. Residential solid fuel burning is also responsible for a quarter of global black carbon emissions (Batchelor et al. 2019). Household air pollution from cooking with traditional solid fuels contributes to more than 23,000 premature deaths in Uganda annually. Approximately 6,800 children also die from acute lower respiratory infections caused by smoke from solid fuels (GACC, 2016).

The unsustainable supply of biomass fuels is slowly leading to the extinction of indigenous wood and shrub species. The additional pressure on land resources to cater for agricultural land, human settlements will soon create an acute shortage in the supply of the long- considered cheap fuel. There is therefore need to explore fast growing sources of bioenergy feedstock to provide energy at a competitive cost with minimal environmental impact. However, using biomass as a feedstock for fuel and chemical production is challenging due to the great amount of innate variability between different biomass types and within individual biomass species. This inconsistency arises from varied growth and harvesting conditions of the biomass, which presents challenges for conversion processes. Moreover, the conversion processes require physically and chemically uniform materials (Williams et al. 2017). Biofuels production is affected by several variables related to biomass composition, including moisture content, ash content, carbohydrate distribution, and higher heating value (Nunes et al.2018). The physiochemical properties of biomass are also important in the design and operation of biomass conversion processing facilities (Cai et al. 2017; Williams et al. 2017).

In this study, over 350 indigenous biomass species in Uganda were reviewed to select biomass suitable for processing into fuel with a high energy density, low ash content and easy ignition (Katende et al. 1995; Tabuti et al. 2003). The following biomass species were selected: *Acacia mearnsii, Broussonetia papyrifera, Lantana camara, Mimosa pigra, Psidium guajava and Senna spectabilis.* Thermochemical conversion of biomass is mainly affected by the reaction conditions and biomass composition. The aim of this study, therefore is to predict the yield of pyrolysis products from the selected biomass using Aspen Plus version 11. To the best of the authors' knowledge, the pyrolysis products for these biomass species have not been simulated using Aspen Plus version 11. The authors also aim to establish the potential of the selected invasive shrub species for bioenergy applications.

2 Materials and Methods

2.1 Materials

The invasive shrubs selected for this study are shown in Table 1 and the sites for sample collection shown in Fig. 1.

Table 1: Selected invasive biomass species

Species	Ecology, District	Remarks
Acacia mearnsii	Kabale district	Mainly found in the steep mountain slopes and is an efficient nitrogen fixer.
Broussonetia papyrifera	Mabira forest, Buikwe district	Invaded Mabira forest extensively and has various medicinal and agro-forestry properties
Lantana camara	Budongo forest reserve, Masindi district	Habitat for tsetse flies and commonly used for firewood
Mimosa pigra	Kaazi, Lake Victoria shore, Wakiso district	Has medicinal properties and can be used for erosion control around water bodies. The leaves have also been used for extraction of Si nanocrystals.
Psidium guajava	Budongo forest reserve, Masindi District	Extensively invaded Budongo and Semuliki National Parks. Its fruit can be eaten raw and it coppices
Senna spectabilis	Mabira forest, Buikwe district	Fast growing and coppicing. Often used as a boundary marker and the wood is termite resistant

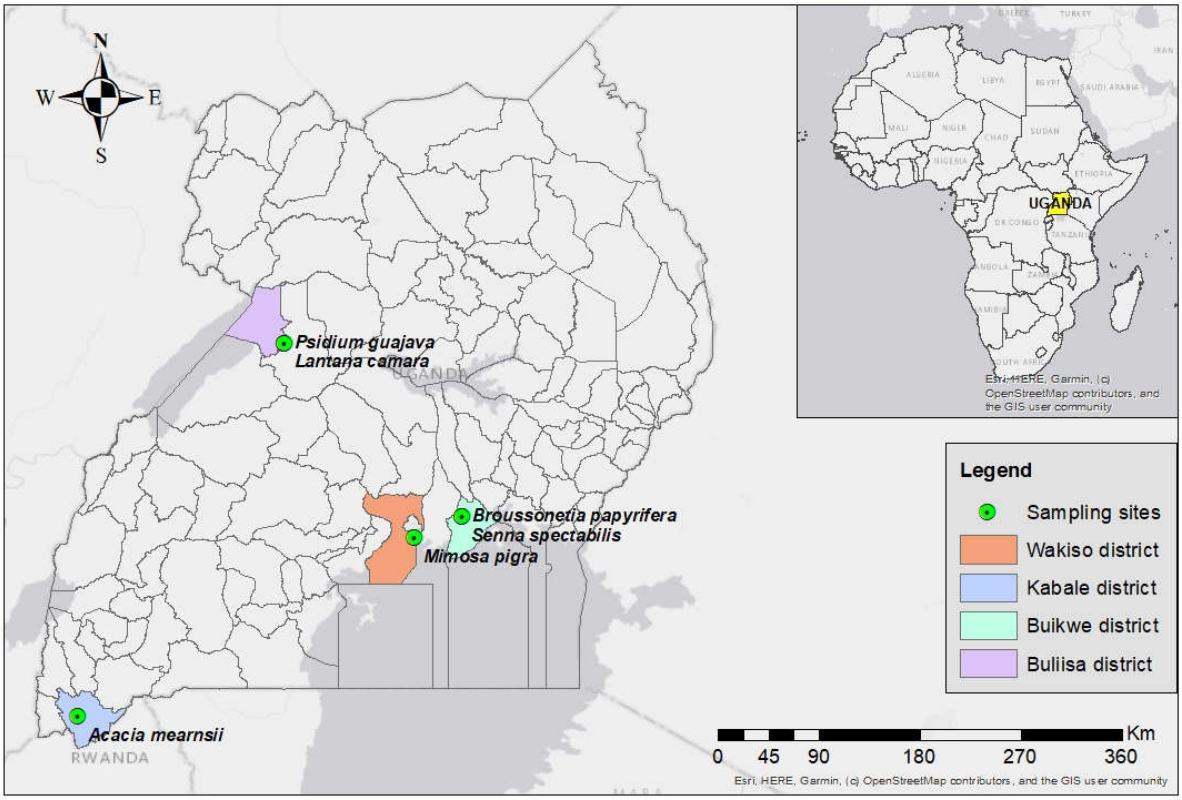

Figure 1: Location of sampling sites

2.2 Sample Collection and Preparation

The invasive shrubs (mainly branches and stems) were collected from wild ecosystems ecologies where they are well established, as shown in Table 1. The samples were sun-dried for two weeks prior to analysis.

2.3 Sample analysis

2.3.1 Proximate analysis

The moisture, ash and volatile content of the biomass samples were determined by using a Thermo-gravimetric analyzer (Eltra Thermostep), following the ASTM E1131-20 standard procedure (ASTM

International, 2020). The ASTM procedure was used to determine proximate values using thermogravimetry. The fixed carbon content is calculated according to equation 2.1.

$$FC(\%) = 100 - (\%Ash + \%VM) \quad (2.1)$$

Where % FC, %Ash and %VM, is the mass percentages of fixed carbon, ash and volatile matter of the raw sample respectively.

2.3.2 Ultimate analysis

The ultimate analysis to determine the Carbon (C), Hydrogen (H) and Sulphur (S) in the biomass was carried out using an ELTRA CHS 580 analyzer following the ASTM D-3176-15 standard procedure (ASTM International, 2015). The nitrogen content was determined by the procedure described by Okalebo et al. (2002). The samples were prepared as recommended and the nitrogen content determined by the colorimetric method at 650 nm. The oxygen content was calculated using the following equation:

$$O(wt\%) = 100(wt\%) - C(wt\%) - H(wt\%) - N(wt\%) - S(wt\%) \quad (2.2)$$

2.3.3 Morphology

The morphology of the samples was examined using a scanning electron microscope (VEGA3, TESCAN). The samples were uncoated due to unavailability of a carbon coater in Uganda at the time of this study. A low voltage of 2.5 kV and low vacuum (chamber pressure of 10^{-1} - 3Pa and 10^{-4} in the gun area) was used for this work (Hummelgård, 2017; JEOL Limited, n.d). The images were processed using Image J software. Single visible pores on the surface were measured to obtain an approximate size of the pores for all the biomass species.

2.3.4 Heating value

The heating value of the biomass was determined using an adiabatic oxygen bomb calorimeter (IKA C2000 automated digital calorimeter) according to the ASTM D5865-13 standard test method.

2.3.5 Thermal properties

Thermal analysis was carried out using a thermo gravimetric analyzer (Eltra-Thermostep) to obtain the weight loss during heating and the derivative thermogravimetry (DTG) to obtain the rate of mass loss. The samples were heated in Nitrogen at a rate of 6 °C/min until a temperature of 1000 °C was reached.

2.3.6 Analysis of micro and macro elements of the biomass

The quality of biomass, which in turn affects the bioenergy products and potential effects on the environment is strongly associated with the organic and inorganic components (Álvarez-Álvarez et al. 2018) .The total phosphorus (P), potassium (K), calcium (Ca), sodium (Na) and magnesium (Mg) in the biomass was determined using procedures described by Okalebo et al. (2002). Total phosphorus was determined colorimetrically at a wave length of 880 nm following complexion with mixed reagent composed of ascorbic acid, potassium antimonyl tartrate and ammonium molybdate. Total potassium, Calcium, and Sodium were determined using a flame photometer. Magnesium, was determined using an Atomic Absorption Spectrophotometer.

2.3.7 Chemical composition

The cellulose, hemicellulose and lignin contents of the biomass were analyzed via Neutral Detergent Fibre (NDF), Acid detergent lignin (ADL) and Acid Detergent Fibre (ADF) methods (Okalebo et al. 2002; Van & Robertson , 1985).

2.3.8 FT-IR analysis

The functional groups in the biomass was analyzed using a JASCO 6600 FT-IR spectrometer. All spectra were recorded in absorption mode in the range of 4000-400 cm^{-1}, at a resolution of 4 cm^{-1}.

2.3.9 Biomass pyrolysis modeling

The pyrolysis of the six biomass species was simulated using ASPENPlus version 11. The composition and yield of the pyrolysis process was modeled by decomposing the biomass into discrete elements (C, H, N, O, S, Cl, ash and moisture).

3 Results and discussion

3.1 Proximate analysis

Proximate analysis is one of the most important characterization methods. This consists of determining moisture, ash, volatile matter and fixed carbon contents of the raw biomass. These values are crucial both for the combustion process and plant design. High moisture values of the biomass decrease the combustion yield, while high volatile matter/fixed carbon ratios are related with the fuel's reactivity. In addition, the ash content influences the transport, handling and management costs of the process. It is also influential in corrosion and slag formation (García et al. 2013).

The proximate analysis of the biomass samples is shown in Table 2. The moisture content of the shrub species varied between 8.26 % - 10.65 %, which corresponds to low moisture content (Patel et al. 2012). The volatile matter for all the shrub species also varied between 71.69% - 75.10 %, therefore *Senna spectabilis* is the most reactive species while *Mimosa pigra* is the least reactive (Lv et al. 2010; Mierzwa-Hersztek et al. 2019; Rocha et al. 2020; Singh et al. 2017). *Senna spectabilis* also had the lowest ash content, hence most suitable for combustion (He et al. 2018; Singh et al. 2017). The fixed carbon content was in the range of 14.25 % -18.20 % for the biomass species. The fixed carbon of a fuel is the percentage of carbon available for char combustion after all the volatile matter is removed from the biomass (Singh et al. 2017).

Table 2: Proximate analysis of selected biomass species

	As received				Dry basis		
Species	**Moisture content (%)**	**Volatile matter (%)**	**Ash (%)**	**Fixed Carbon (%)**	**Volatile matter (%)**	**Ash (%)**	**Fixed carbon* (%)**
Acacia mearnsii	8.74±0.12	72.01±1.11	1.05±0.34	18.20±0.66	78.31±1.12	1.14±0.37	20.55±0.77
Broussonetia papyrifera	8.31±0.15	75.10±0.44	0.83±0.22	15.76±0.11	81.34±0.37	0.90±0.24	17.76±0.17
Lantana camara	8.23±0.05	72.53±0.16	1.71±0.19	17.53±0.29	78.50±0.19	1.85±0.21	19.65±0.31
Mimosa pigra	8.26±0.19	71.69±0.79	1.88±0.19	18.17±0.42	77.61±0.73	2.03±0.21	20.36±0.51

Species	As received				Dry basis		
	Moisture content (%)	Volatile matter (%)	Ash (%)	Fixed Carbon (%)	Volatile matter (%)	Ash (%)	Fixed carbon* (%)
Psidium guajava	9.23±0.23	72.12±0.33	0.92±0.15	17.73±0.36	78.77±0.30	1.01±0.17	20.22±0.41
Senna spectabilis	10.65±0.63	75.10±0.91	-	14.25±0.49	83.29±1.08	-	16.71±0.56

* calculated value (%)

3.2 Ultimate analysis

Biomass fuel efficacy and emissions during combustion is determined by its Carbon, Hydrogen, Oxygen and Nitrogen content (Meng, et al. 2020; Singh et al. 2017). The ultimate analysis for the shrub species is shown in Table 3. Carbon content was highest in the bark of *Acacia mearnsii* (50.34 %), and lowest in *Lantana camara* (35.23%). The oxygen content was highest in *Lantana camara* and lowest in *Senna spectabilis* bark. The Nitrogen and Sulphur content is in range with most biomass species as reported by other authors (López , 2016; Tripathi et al.2016; Tursi, 2019). There are also variations in the chemical composition for previously studied species like *Acacia mearnsii, Broussonetia papyrifera*, *Lantana camara* and *Mimosa pigra* (Badan et al. 2020; Havilah et al. 2016; Kosowska-Golachowska et al. 2018; Wongsiriamnuay & Tippayawong, 2010). This can be attributed to the different growing conditions of the plants such as climate, soil type, soil pH, nutrients and geographical location.

Table 3: Ultimate analysis of selected biomass

No.	Species	Carbon (C) %	Hydrogen (H) %	Nitrogen (N) %	Sulphur (S) %	Oxygen (O)* %
1	*Acacia mearnsii bark*	50.34	4.02	1.43	-	44.21
2	*Acacia mearnsii wood*	47.96	6.29	0.09	-	45.66
3	*Broussonetia papyrifera bark*	44.56	6.81	1.07	-	47.56
4	*Broussonetia papyrifera wood*	47.58	6.13	0.09	-	46.20
5	*Lantana camara*	35.23	4.54	1.31	0.80	58.12
6	*Mimosa pigra*	41.97	5.12	0.55	0. 93	51.43
7	*Psidium guajava*	42.30	5. 96	0.64	0. 38	50.72
8	*Senna spectabilis bark*	47.98	4.69	5.10	3.10	39.13
9	*Senna spectabilis wood*	47.35	6.59	0.28	-	45.78

* calculated value

3.3 Morphology

The surface morphology of the different shrub species is shown from Fig. 2 and a summary of the surface pore diameters in Table 4. *Acacia mearnsii* and *Psidium guajava* exhibited a dense and integrated structure with miniscule pits on the surface, and the least diameter measured. *Broussonetia papyrifera, Senna spectabilis* and *Lantana camara* had irregularly shaped pores distributed throughout the surface Additionally, *Mimosa pigra* has comparatively lateral pits on the surface and the differences in the morphologies between the biomass species is attributed to their different compositions (Kanbayashi & Miyafuji, 2016).

Table 4: Diameter of surface pores on selected biomass species

No.	Species	Diameter, µm
1	*Acacia mearnsii*	8.99 ± 1.65
2	*Brusonetia papyrifera*	36.35 ± 26.00
3	*Lantana camara*	26.14 ± 12.46
4	*Mimosa pigra*	18.44 ± 7.00
5	*Psidium guajava*	7.52 ± 2.64
6	*Senna spectabolis*	21.47 ± 8.05

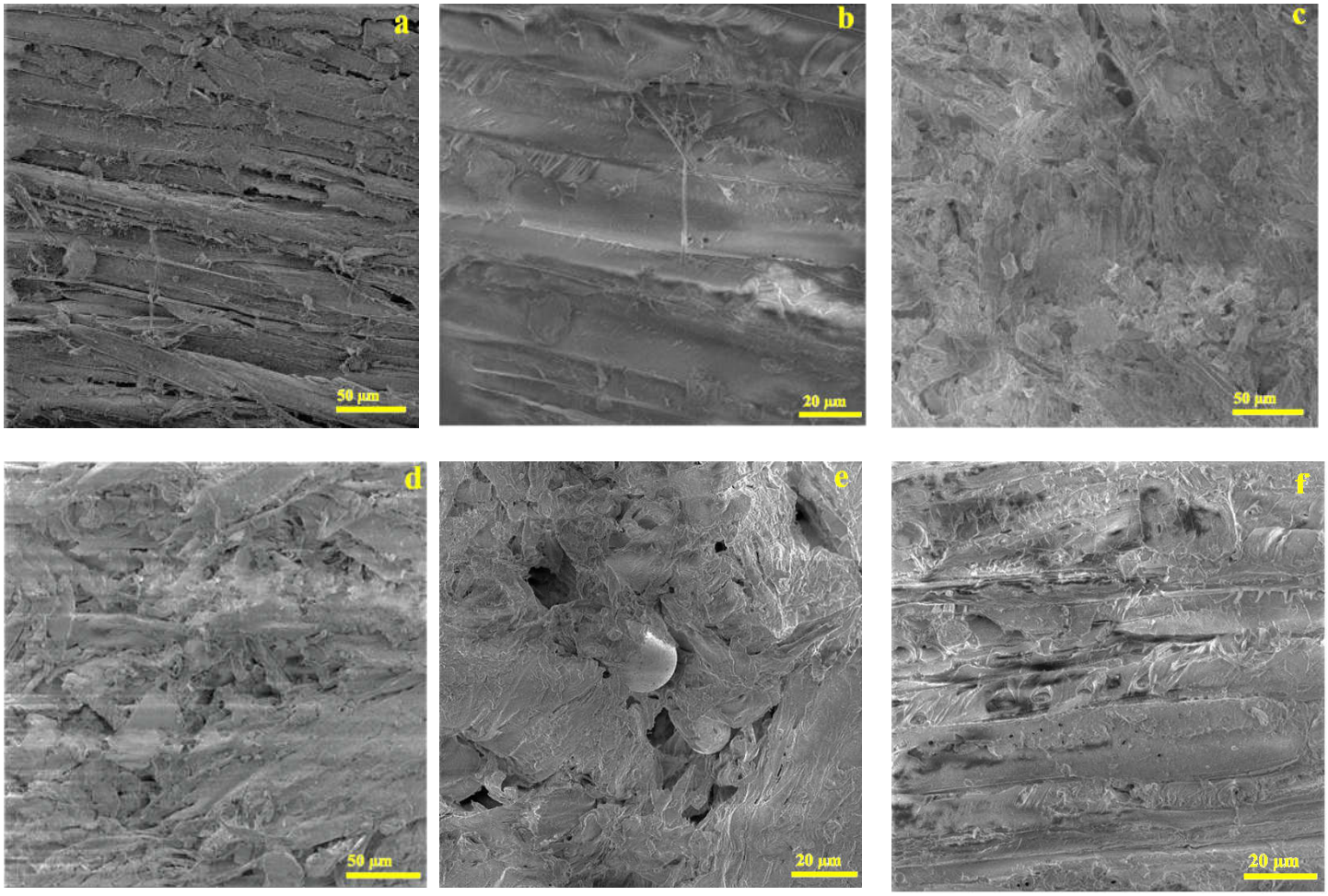

Figure 2: Morphology of the biomass species (a) *Mimosa pigra* (b) *Acacia mearnsii* (c) *Broussonetia papyrifera* (d) *Lantana camara* (e) *Senna spectabilis* (f) *Psidium guajava*.

3.4 Micro and Macro nutrients of biomass

Biomass contains inorganic substances usually referred to as ash, in traces, whose quantity depends on the type of raw material. The most common elements are calcium, sodium, potassium, magnesium, phosphorus, silicon, aluminum and iron (Tursi, 2019). The inorganic matter for the selected biomass is shown in Table 5 and the order of concentration is agreeable with works from other authors (Abián et al. 2017; Tsuchiya et al. 2010). Calcium is the most predominant element in all species but has been reported not to have an influence on the pyrolysis and devolatilization processes of biomass (Abián et

al. 2017). All the biomass species have an ash content below 5 % and therefore no slagging is expected to occur during gasification and combustion (Kumar & Anand, 2019).

Table 5: Inorganic matter in selected biomass species

No.	Species	Potassium (K) %	Calcium (Ca) %	Magnesium (Mg) %	Sodium (Na) %
1	*Acacia mearnsii*	0.12	2.17	0.73	0.62
2	*Broussonetia papyrifera*	0.34	2.17	0.74	0.62
3	*Lantana camara*	0.71	2.48	0.86	0.62
4	*Mimosa pigra*	0.19	1.55	0.55	0.47
5	*Psidium guajava*	0.19	0.93	0.33	0.31
6	*Senna spectabilis*	0.31	2.48	0.82	0.78

3.5 Chemical composition

The chemical composition of the shrub species is shown in Table 6. Cellulose is the main component for all the shrub species, varying slightly between each type of biomass. This shows that all the species are suitable for biofuel production (Cavalaglio et al. 2020). Research also shows that the cellulose and lignin contents of biomass affect pyrolysis and gasification. Additionally, the pyrolysis rate is higher for biomass with higher cellulose content, while it is slower for biomass with higher lignin content (Gani & Naruse, 2007; Lv et al. 2010; Shahbaz et al. 2022).

The cellulose content in the biomass also enhances the ignition characteristics and decomposition of lignin, since cellulose compounds have branching chains of polysaccharides and no volatile aromatic compounds (Gani & Naruse, 2007). Consequently, the biomass will burn in the following steps. First, the cellulose components in the biomass are volatilized, so that the porosity in the char particles of biomass increases and that oxygen easily diffuses into the char particles. Next, the lignin components in the biomass can also react with oxygen diffused even if the reactivity of lignin itself is low. The chemical composition of biomass further affects gasification by changing the char structure, and the char from biomass with higher lignin content has higher porosity and reactivity (Lv et al. 2010). Therefore, from the results in Table 5, *Senna spectabilis* is most suitable for fast pyrolysis and *Mimosa Pigra* is the best for production of char with high porosity. Biomass with higher lignin coefficient is also expected to produce more hydrogen, thus it is more suitable for hydrogen production by gasification (Tian et al. 2017). *Mimosa pigra* has the highest lignin concentration and therefore more suitable for production of hydrogen.

Table 6: Chemical composition of selected biomass

No.	Species	Cellulose /wt %	Hemicellulose /wt %	Lignin /wt%
1	*Acacia mearnsii*	40.20	21.33	14.71
2	*Brusonetia papyrifera*	41.18	24.35	19.61
3	*Lantana camara*	47.06	22.37	13.73
4	*Mimosa pigra*	41.59	17.02	21.78
5	*Psidium guajava*	47.06	16.51	19.61
6	*Senna spectabilis*	48.04	19.45	16.67

3.6 FT-IR analysis

The functional groups present in the biomass samples are identified by the FTIR spectrum of the biomass species shown in Fig.3. Transmission bands are typical for lignocellulosic biomass, but the intensities vary due to differences in composition of the biomass species. The functional group assignments for the peaks are comprehensively discussed elsewhere and only a few are discussed here (Dobrica et al. 2008; Li et al. 2018; Nandiyanto et al. 2019; Xu et al. 2013; Yang et al. 2020). The peak at 1508 cm^{-1} shows the C=C- C aromatic ring stretching and vibration associated with lignin. The intensity of this peak is sharpest for *Mimosa pigra* that has the highest lignin content. Also, the peak at 1032 cm^{-1} is assigned to C-O stretching, aromatic C-H in plane deformation associated with cellulose and lignin and it exists for all samples. Further still, the peak at 1315 cm^{-1} assigned to the O-H in plane bending of cellulose and hemicellulose. The peak at 1730 cm^{-1} is assigned to the C=O stretching in the acetyl group and carboxylic acid, associated with the presence of hemicellulose. The biomass species are all unprocessed and the differences in peak intensities are caused only by the difference in composition of cellulose, hemicellulose, and lignin.

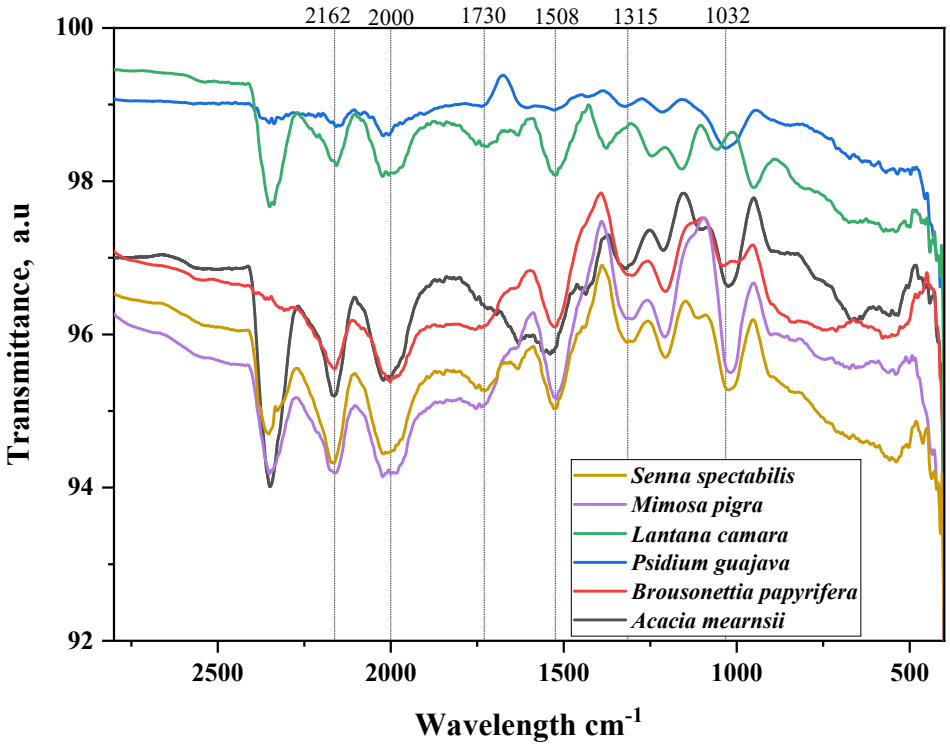

Figure 3: FTIR spectra for selected biomass

3.7 Calorific value

The calorific values of the selected biomass species are shown in Table 7. The higher heating values are similar between the biomass species except *Lantana camara* which has the lowest value that can be correlated to its low lignin content as shown in Table 5 (Demirbas, 2002) . Moreover, the calorific values of the selected biomass are lower than those reported for similar biomass in open literature (Ivanova et al. 2018; Kosowska-Golachowska et al. 2018; Kumar et al. 2009; Mundike et al. 2017). The calorific values for the selected biomass are comparable to the energy content of woody species such as poplar (17.07 MJ/kg),birch (18 MJ/kg) and agricultural residues like wheat straw (17 MJ/kg) and rice husk (16 MJ/kg) (Chai et al. 2021; Ioelovich 2018; Osman et al. 2021).

Table 7: Heating value of selected biomass species

No.	Species	Higher Heating value (MJ/kg)
1	*Acacia mearnsii*	17.66 ± 0.09
2	*Brusonetia papyrifera*	17.70 ± 0.11
3	*Lantana camara*	16.87 ± 0.02
4	*Mimosa pigra*	17.42 ± 0.35
5	*Psidium guajava*	17.26 ± 0.17
6	*Senna spectabolis*	17.84 ± 0.14

3.8 Thermal analysis

The TGA and DTG curves for the biomass samples are shown in Fig. 4 and a summary of the weight loss, onset temperature (T_i), final temperature (T_f) and peak temperature (T_p) of the two stages of thermal decomposition in Table 8. The first stage of thermal decomposition is the moisture loss stage and the second stage is the decomposition of the biopolymer components (cellulose, hemicellulose and lignin). The weight loss in the first stage is due to the elimination of moisture in the temperature range of 23 °C -108 °C. The steep weight loss in the second stage is in the range of 79 % - 88 % for the biomass species but is higher for samples with a higher content of hemicellulose and cellulose (Haldar & Purkait, 2020). The mass loss is also associated with the release of CO_2 and CH_4 from the decomposition of biopolymers, as well as release of chemically bonded CO_2 and water (Yguatyara de Luna et al. 2019). From approximately 600 °C -900 °C, the mass loss rate drops due to evolution of carbon containing species (CO_X, C_xH_y and tars) and char oxidation until a constant weight is achieved (García et al. 2013). The peak temperature from the DTG curve, which corresponds to the active decomposition of cellulose, is in the range of 455°C- 495°C for all the biomass species. The peak temperatures are higher than those reported in open literature for woody biomass (350°C) (García et al. 2013; Wang et al. 2021).

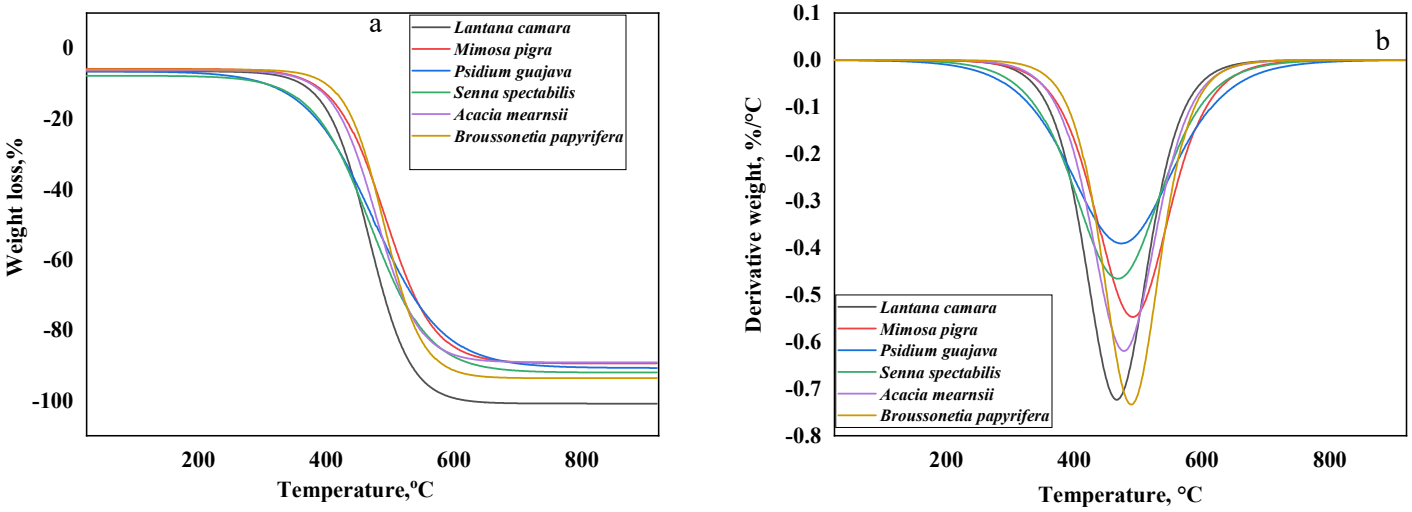

Figure 4: (a) TGA and (b) DTG curves for the selected biomass

Table 8: Summary of TGA data

	Moisture loss			Thermal decomposition			
Samples	**Δ m, %**	**T_i, °C**	**T_f, °C**	**Δ m, %**	**T_i, °C**	**T_f, °C**	**Tp, °C**
Acacia mearnsii	11.55	23.15	106.41	79.11	395.35	556.63	482.21
Brusonetia papyrifera	12.84	25.40	104.15	82.28	426.42	573.64	494.66

Lantana camara	14.28	23.14	107.69	87.92	372.45	544.51	467.78
Mimosa pigra	8.21	24.59	104.11	82.38	251.42	593.02	494.66
Psidium guajava	8.76	23.98	106.18	81.77	287.64	612.60	473.40
Senna spectabolis	12.53	25.40	106.41	81.43	343.15	644.12	454.50

3.9 Modeling of biomass pyrolysis using ASPENPlus

The biomass pyrolysis model used in this study is shown in Fig. 5. The following assumptions were made for the modeling process in ASPENPlus version 11;

(1) Pyrolysis was carried out in a Gibbs reactor, hence reaction kinetics were not specified.
(2)The volume of the reactor is 0.09 m^3.
(3) Both gases and solids obeyed the ideal gas law.
(4) The biomass particles had uniform temperature distribution and size.
(5)The reactor was under constant pressure of 0.2 MPa
(6) The reaction equilibrium is calculated by minimizing the Gibbs free energy.
(7) Both gases and solids are assumed to be in thermal equilibrium and create a homogenous mixture.
(8)The feedstock was specified according to the Proximate and Ultimate analysis of the biomass shown in Table 2 and 3 respectively.
(9) For all simulations, a biomass feeding rate of 125 kg/h was employed.
(10) The chemical composition of the bio-oil included five broad categories of compounds; hydroxyaldehydes, hydroxyketones, sugars and dehydrosugars, carboxylic acids and phenolic compounds (Chen, 2015; Mohan et al. 2006)
(11) The product from pyrolysis were analyzed based on temperature and residence times. The pyrolysis of the six biomass species were simulated at 350 °C for 1 h of solid residence time, 650 °C for 0.5 h of solid residence time and 800 °C for 60 s of solid residence time. The product yields were expressed as a weight percentage of the total amount of pyrolysis products.

The products of pyrolysis for the biomass species at different temperatures is shown in Fig.6. At the temperatures investigated, biogas and biochar are the main products of all the biomass samples pyrolysed. For all species of biomass, the yield of biogas increased as the temperature increased from 350 °C - 800 °C. The highest yield of conversion to biogas was predicted for *Lantana camara* (93 %), followed by *Mimosa pigra* (84 %), *Psidium guajava* (84 %), *Broussonetia papyrifera* (80 %), *Acacia Mearnsii* (73 %), and *Senna spectabilis* (71 %) at 800 °C. The gaseous products increase at higher temperatures due to the formation of secondary cracking reactions of the pyrolysis vapors and secondary decomposition of biochar, producing non-condensable gaseous substances (Chiodo et al. 2016). Additionally, the biochar yield decreased with an increase in temperature from 350 °C - 800 °C for all the biomass. The highest biochar yield conversion is projected for *Senna spectabilis* (39 %), followed by *Acacia Mearnsii* (38 %), *Broussonetia papyrifera* (33 %), *Psidium guajava* (31 %), *Lantana camara* (24 %) and *Mimosa pigra* (24%). Yu et al. (2019) observed a reduction in biochar yield from 32 % at 350 °C to 21 % at 600 °C for Hinoki cypress. Additionally, Li et al. (2021) reported a 49 % conversion of raw maize straw to biochar at 350 °C. Consequently, this study confirms findings in literature suggesting that the typical biochar yield during slow pyrolysis is 35 % by weight and decreases with increase in temperature (Li et al. 2022; Tomczyk et al. 2020).

The bio-oil yield was the lowest among the products of pyrolysis, but it increased as the temperature increased. The highest bio-oil yield conversion is projected for *Senna spectabilis* (2 %), followed by *Psidium guajava* (0.4%), *Mimosa pigra* (0.4 %), and *Lantana camara* (0.3 %) at 800 °C. There is no bio-oil conversion at 800 °C for *Acacia Mearnsii and Broussonetia papyrifera*. There are numerous factors that affect bio-oil formation such as biomass composition, reaction time and temperature, heating rate, feed rate and vapor residence time. The yields of bio-oil from woody biomass are typically

in the range of 60-95 wt %, depending on the feedstock composition (Tomczyk et al. 2020). Therefore, the bio-oil conversion from the selected biomass is much lower than expected mainly because of its composition.

The moisture in the biomass for all the species is extracted by 108 °C from the TGA analysis in Fig. 4, therefore the water produced from 350 °C - 800 °C is attributed to different tar productions (Li et al. 2021). The yield of the liquid products decreases with an increase in temperature, due to secondary decomposition of tar products at high temperatures (Chen et al. 2021; Li et al. 2021; Neves et al. 2011). The highest liquid product yield is predicted for *Broussonetia papyrifera* (29 %), *Psidium guajava* (25 %), *Mimosa pigra* (23 %), *Lantana camara* (23 %), *Senna spectabilis* (21 %), and *Acacia Mearnsii* (21%) at 350 °C. Peters et al. (2017) simulated the liquid yield of beech wood at 520 °C, and obtained a yield of 29 % from the simulation in ASPENPlus and experiments. The results from this work are therefore in agreement with findings in literature.

The common trend of the concentration of the gas components; Hydrogen (H_2), Carbon monoxide (CO), Carbondioxide (CO_2), and water (H_2O) for the biomass samples are shown in Fig.7 (a). The concentration of CO and H_2 increased with increasing temperature. The increases in the CO, H_2 content relates to the decreasing concentrations of CO_2, and H_2O as reported previously in literature (Lan et al. 2022). Also, the concentrations of the light hydrocarbons; C_6H_{12}, C_8H_{16}, C_9H_{18}, $C_{10}H_{20}$, C_7H_{14}, C_5H_{10} decreases with increase in temperature, which results in increase of H_2 concentrations (Lestinsky & Palit, 2016).

CO_2 is formed more rapidly at higher temperatures than CO, so as the temperature increases from 350 °C to 800 °C, CO content decreases and the CO_2 content increases. This is because higher temperatures are beneficial for the oxidation and reduction reactions (Lan et al. 2022).

Biomass fuel combustion is also reported to result in Nitrous oxides (NO_X) and Sulphur oxides (SO_X emissions (Li et al. 2021). NO_x emissions arise from atmospheric nitrogen and from fuel-bound nitrogen, which is released during both the devolatilization and the char oxidation phases (Li et al. 2021; Rokni et al. 2018). The oxidation of fuel-bound Sulfur is the only source of SOx emissions (Wang et al. 2019). Sulfur oxides were not present in the biomass species without Sulphur as shown in Table 3. Additionally, no hydrogen chloride (HCl) emissions were observed from any of the biomass species. This means they can all be used in fuel blends without creating problems such as deposition in boilers and corrosion. From Fig.7 (b), the SO_2 increase with increase in temperature up to 600 °C and then reduce at 800 °C. The SO_3 emissions also follow the same trend. Li et al. (2020) observed that the concentration of SO_2 was highest at 600 °C during the pyrolysis of corn straw and it reduced with further increase in temperature. The Sulphur oxides emissions reduce at higher temperatures due to the depletion of volatiles and adsorption of ash alkali earth metals (Li et al. 2020). The NO_2 emissions increased with increase in temperature while the NO emissions reduced with increase in temperature. This is in agreement with the findings of Shao et al. (2013) that as the temperature increases, the formation of NO is inhibited due to increase in the combustion rate that hinders the formation of intermediates of combustion. Consequently, the simulation results show that the yields of the pyrolysis products will vary with the changes in reaction temperature, residence time and feedstock.

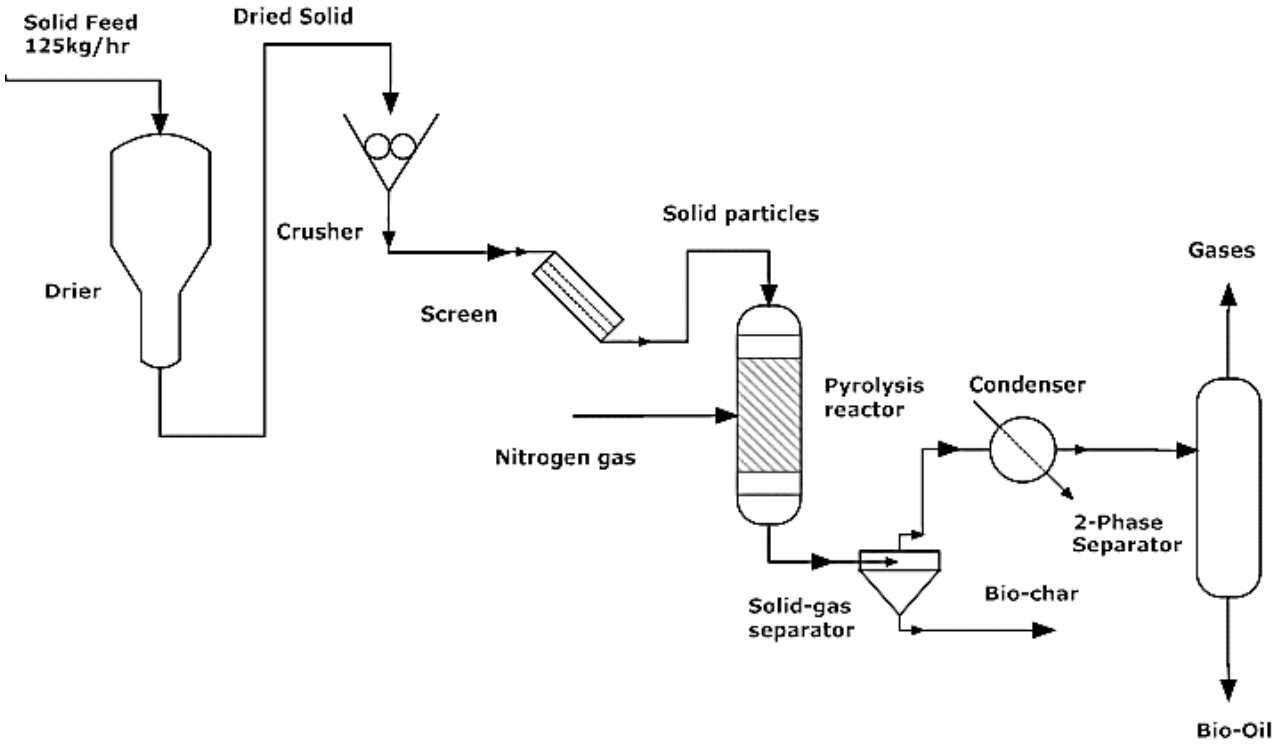

Figure 5: Simulation flow chart of biomass pyrolysis process

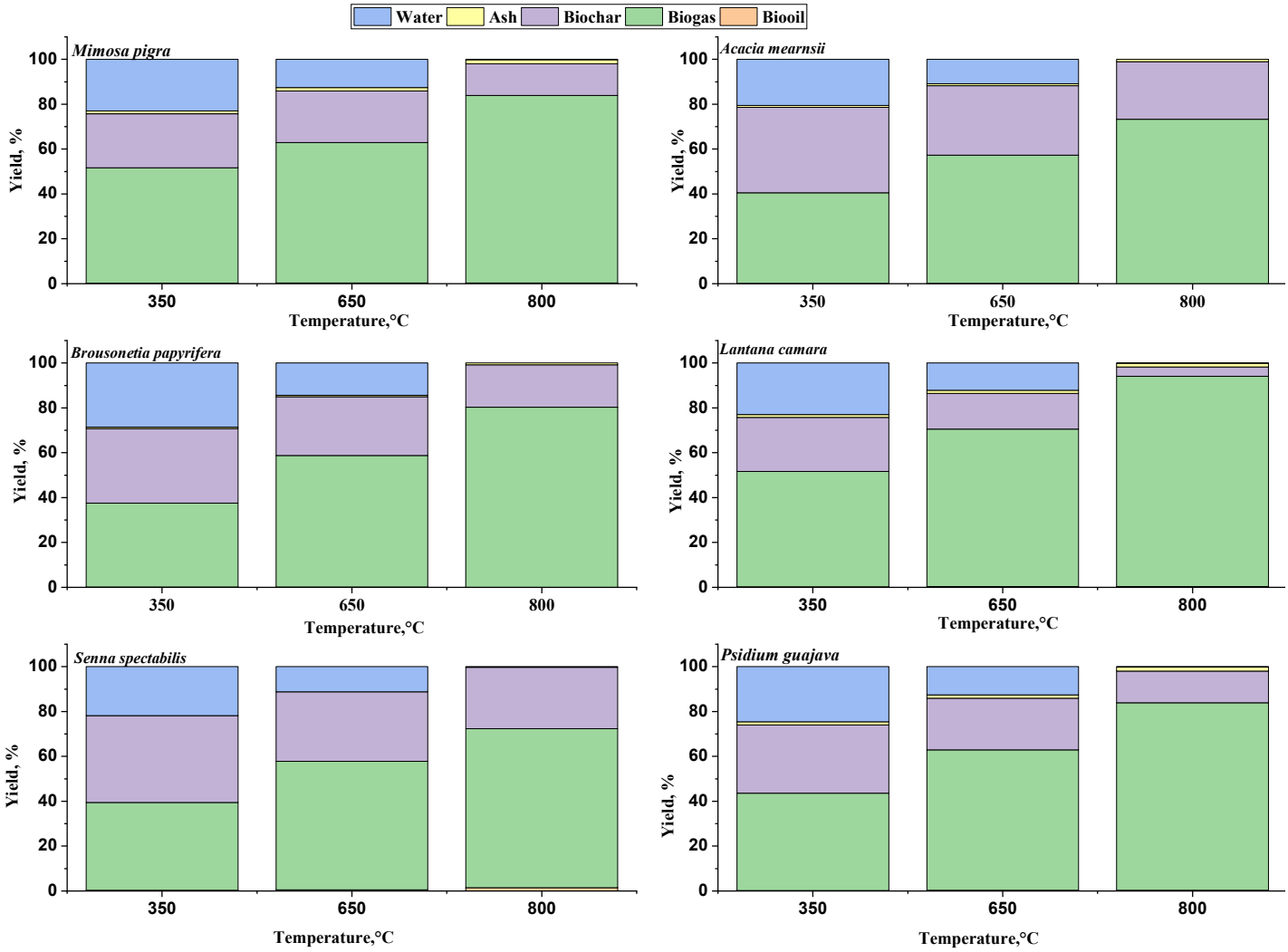

Figure 6: Yield of pyrolysis products for selected species at different temperatures

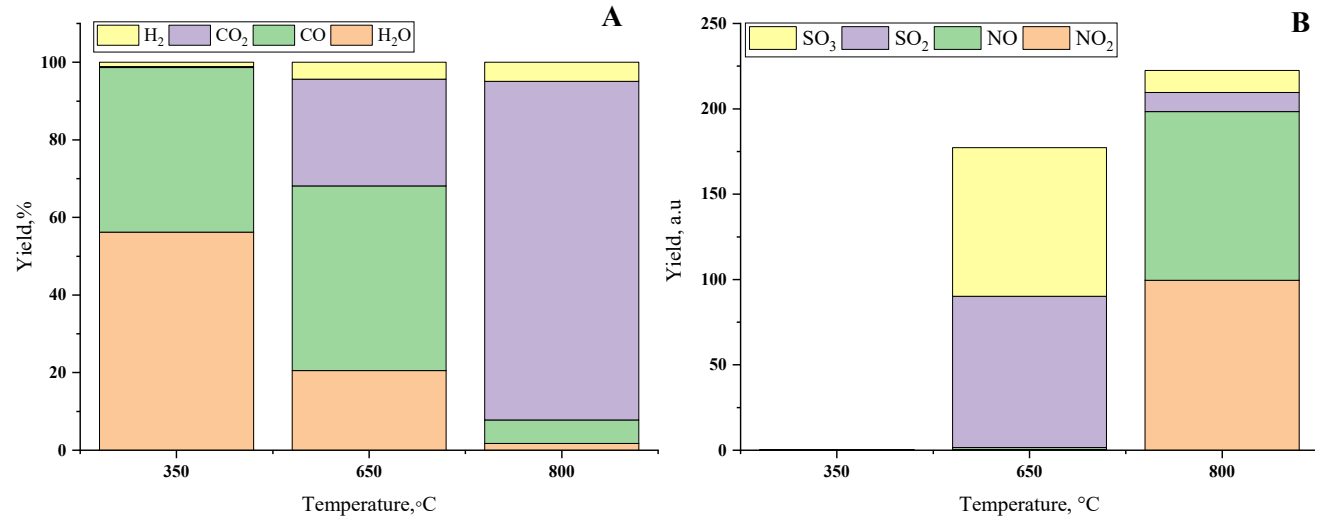

Figure 7: Gas yields from selected biomass (a) gas products (b) gaseous emissions

4 Conclusion and future perspectives

This study focused on characterization of six biomass species as alternative feedstock for energy use. From the results, all the shrubs are suitable for thermochemical and biochemical conversion processes. The lignocellulosic biomass was also found to have different physicochemical characteristics and therefore classified to suit selected conversion processes. *Senna spectabolis* had the highest heating value of 17.84 MJ/kg, volatile matter (83.29 % dry basis) and least ash content, and is therefore the most suitable for energy conversion. The structure of the raw biomass was studied using Fourier transform infrared spectroscopy (FTIR) and Scanning electron microscopy (SEM). The FTIR spectra for all the biomass was typical for lignocellulosic materials but the intensities of the peaks differed with chemical composition of the samples. The SEM images obtained for all biomass were clear despite the samples being uncoated, and the differences in surface morphologies of the samples were observed. The thermal analysis of the raw biomass samples also revealed that they are thermally stable with the highest peak temperature of 495 °C observed for *Broussonetia papyrifera* and *Mimosa pigra.* Furthermore, the pyrolysis of the biomass species was also successfully simulated using Aspen Plus version 11. The yields of biochar, bio-oil and biogas from all the six species were obtained for slow (350 °C), fast (650 °C) and flash pyrolysis (800 °C) at 1h, 0.5h and 60 s of solid residence time respectively. The pyrolysis product yields from the simulation were in agreement with observations recorded in literature, and therefore the results can be used as a basis for further designs utilizing the investigated feed stocks. The main product of pyrolysis was biogas, realizing the highest yield of 93 % for *Lantana camara* at 800 °C. The highest yield of biochar is achieved at 350 °C and the maximum conversion of 39 % is observed for *Senna spectabilis.* The bio-oil yield from the investigated biomass was low, despite employing the accepted pyrolysis conditions for optimum yield. Future Biorefinery designs therefore will focus on optimizing biogas and biochar yields from the biomass. The NO_X and SO_X emissions from pyrolysis of the biomass was also profiled. Although the quantities of the emissions predicted are small, emission control measures should be incorporated into industrial scale designs and pretreatment of the biomass can be considered to increase combustion efficiency.

5 Statements and declarations

5.1 Funding

This work was supported by the African Center of Excellence in Materials, Product Development and Nanotechnology (MAPRONANO ACE) funded by the World Bank and Government of Uganda [Project Identification P151847, IDA Number 5797-UG].

5.2 Acknowledgements

The authors also acknowledge the Materials and metallurgy laboratory, Busitema University, Tororo, Uganda, for conducting the FT-IR and SEM experiments. Naturinda Evet is also credited for the GIS map.

5.3 Conflict of interest

The authors declare no conflict of interest.

5.4 Author contributions

Conceptualization, Methodology, formal analysis and investigation, and original draft preparation: [Ayaa Fildah]; review and editing: [Michael Lubwama, John Baptist Kirabira and Xi Jiang]; Funding acquisition and supervision: [Michael Lubwama, John Baptist Kirabira and Xi Jiang].

6 References

1. Abián, M., Alzueta, M., Carvalho, A., Rabacal, M., & Costa, M. (2017). On the role of potassium and calcium on the combustion characteristics of biomass obtained from thermogravimetric experiments. *Energy and Fuels, 31*(11), 12238-12246. doi:10.1021/acs.energyfu.
2. Álvarez-Álvarez, P., Pizarro, C., Barrio-Anta, M., Cámara-Obregón, A., Bueno, J. L., Álvarez, A., Gutiérrez, I., Burslem, D. F. (2018). Evaluation of Tree Species for Biomass Energy Production in Northwest Spain. *Forests, 9*(4),160. doi:https://doi.org/10.3390/f9040160.
3. ASTM International. (2015). ASTM D3176-15 Standard Practice for Ultimate Analysis of Coal and Coke. ASTM International, Pennsylvania. doi:10.1520/D3176-15.
4. ASTM International. (2020). ASTM E1131-20 Standard Test Method for Compositional Analysis by Thermogravimetry. ASTM International, Pennsylvania. doi: 10.1520/E1131-20
5. Badan, P., Thepchatri, T., Tanavat, E., Haruthaithanasan, M., & Haruthaithanasan, K. (2020). Fuel Properties of Some Native Tree Species for Biomass Energy in Thailand. *Thai Journal of Agricultural Science, 53*(1), 53-57.
6. Batchelor, S., Brown, E., Scott, N., & Leary, J. (2019, April 26). Two Birds, One Stone—Reframing Cooking Energy Policies in Africa and Asia. *Energies, 12*(9),1591. doi:10.3390/en12091591
7. Cai, J., He, Y., Yu, X., Banks, S. W., Yang, Y., Zhang, X., Yu,Y., Bridgwater, A. V. (2017). Review of Physicochemical Properties and Analytical Characterization of Lignocellulosic Biomass. *Renewable and Sustainable Energy Reviews, 76*, 309-322. doi:https://doi.org/10.1016/j.rser.2017.03.072
8. Cavalaglio, G., Cotana, F., Nicolini, A., Coccia, V., Petrozzi, A., Formica, A., & Bertini , A. (2020). Characterization of Various Biomass Feedstock Suitable for Small-Scale Energy Plants as Preliminary Activity of Biocheaper Project. *Sustainability, 12*(16), 6678. doi: https://doi.org/10.3390/su12166678
9. Chai, M., Xie, L., Yu, X., Zhang, X., Yang, Y., Rahman, M. M.,Blanco, P. H., Liu ,R., Bridgwater A.V., Cai, J. (2021). Poplar wood torrefaction: Kinetics, thermochemistry and implications. *Renewable and Sustainable Energy Reviews, 143*, 110962. doi:https://doi.org/10.1016/j.rser.2021.110962
10. Chen, D., Cen, K., Cao, X., Chen, F., Zhang, J., & Zhou, J. (2021). Insight into a new phenolic-leaching pretreatment on bamboo pyrolysis: Release characteristics of pyrolytic volatiles, upgradation of three phase products, migration of elements, and energy yield. *Renewable and Sustainable Energy Reviews, 136,* 110444. doi:https://doi.org/10.1016/j.rser.2020.
11. Chen, H. (2015). Lignocellulose biorefinery product engineering. In *Lignocellulose Biorefinery Engineering. Principles and Applications* (1st ed., pp. 125-165). Woodhead Publishing. doi:https://doi.org/10.1016/B978-0-08-100135-6.00005-3
12. Chiodo, V., Zafarana, G., Maisano, S., Freni, S., & Urbani, F. (2016). Pyrolysis of different biomass: Direct comparison among PosidoniaOceanica, Lacustrine Alga and White-Pine. *Fuel, 164*, 220-227. doi:http://dx.doi.org/10.1016/j.fuel.2015.09.093
13. Chirambo, D. (2016). Addressing the renewable energy financing gap in Africa to promote universal energy access: Integrated renewable energy financing in Malawi. *Renewable and Sustainable Energy Reviews, 62*, 793-803. doi:https://doi.org/10.1016/j.rser.2016.05.046
14. Demirbas, A. (2002). Relationships Between Heating Value and Lignin, Moisture, Ash and Extractive Contents of Biomass Fuels. *Energy exploration and exploitation, 20*(1), 105-111. Retrieved 25 January, 2021, from https://journals.sagepub.com/doi/pdf/10.1260/014459802760170420
15. Dobrica, I., Bugheanu, P., Stanculescu, I., & Ponta, C. (2008). FTIR spectral data of wood used in Romanian traditional village constructions. *Analele Universităţii din Bucureşti–Chimie*, *17*(1), 33-39.
16. GACC. (2016). *Uganda Country Profile*. Retrieved 24 January, 2020, from Global Alliance for Clean Cookstoves: http://cleancookstoves.org/country-profiles/focus-countries/8-uganda.html

17. Gani, A., & Naruse, I. (2007). Effect of cellulose and lignin content on pyrolysis and combustion characteristics for several types of biomass. *Renewable Energy, 32*, 649-661. doi:10.1016/j.renene.2006.02.017
18. García, R., Pizarro, C., Lavín, A. G., & Bueno, J. L. (2013). Biomass Proximate Analysis using Thermogravimetry. *Bioresource Technology, 139*, 1-4. doi:10.1016/j.biortech.2013.03.197
19. Haldar, D., & Purkait, M. K. (2020). Thermochemical pretreatment enhanced bioconversion of elephant grass (Pennisetum purpureum): insight on the production of sugars and lignin. *Biomass Conversion and Biorefinery, 12*, 1125–1138. doi:https://doi.org/10.1007/s13399-020-00689-y
20. Havilah, P. R., Sharma, P. K., & Gopinath, M. (2016). Combustion characteristics and kinetic parameter estimation of Lantana camara by thermogravimetric analysis. *Biofuels, 10*(3), 365-372. doi:10.1080/17597269.2016.1259521
21. He, X., Liu, Z., Niu, W., Yang, L., Zhou, T., Qin, D., & Niu, Z. (2018). Effects of pyrolysis temperature on the physicochemical properties of gas and biochar obtained from pyrolysis of crop residues. *Energy, 143*, 746–756.
22. Hummelgård, M. (2017). How to SEM-image untreated / uncoated non-conductive samples in high vacuum by beam-energy charge balancing. Retrieved 28 January, 2021, from https://www.linkedin.com/pulse/howto-sem-image-untreated-uncoated-non-conductive-high-hummelg%C3%A5rd/
23. IEA. (2016B). *http://www.worldenergyoutlook.org*. Retrieved 5 June 2016, from http://www.worldenergyoutlook.org/resources/energydevelopment/energyaccessdatabase/.
24. IEA. (2019). *World Energy outlook.* Retrieved November, 2020, from SDG7: Data and projections : https://www.iea.org/reports/sdg7-data-and-projections/access-to-clean-cooking#abstract
25. Ioelovich, M. (2018). Energy Potential of Natural, Synthetic Polymers and Waste Materials - A Review. *Academic journal of polymer science, 1*(1), 1-15.
26. Ivanova, T., Hernández, A. H., Bradna, J., Cusimamani, E. F., & Montoya, J. C. (2018). Assessment of Guava (Psidium Guajava L.) Wood Biomass for Briquettes' Production. *Forests, 9*(10), 613. doi:10.3390/f9100613
27. JEOL Limited. (n.d.). *Scanning Electron Microscope A to Z. Basic Knowledge for using the SEM.* Retrieved 19 January 2021, from https://www.stcloudstate.edu/cmia/_files/documents/sem-basic-knowledge.pdf
28. Kanbayashi, T., & Miyafuji, H. (2016). Microscopic Investigations on Woody Biomass as Treated with Ionic Liquids. In S. G. Stanciu (Ed.), *Microscopy and analysis* (pp. 203-220). Intechopen. doi:DOI: 10.5772/62721
29. Katende, A. B., Birnie, A., & Tengnas, B. (1995). *Useful trees and shrubs for Uganda. Identification, propagation and management for agricultural and pastoral communities* (Vol. Series 10). (B. Tengnas, Ed.) Kampala: Regional Land Management Unit,Swedish International Development Cooperation Agency (Sida).
30. Kosowska-Golachowska, M., Luckos, A., Magdziarz, A., & Wolski, K. (2018). A study into the combustion process of Acacia mearnsii (black wattle) in a circulating fluidized bed. *23rd International Conference on FBC*, (pp. 1043-1052). Seoul, Korea.
31. Kumar, R. M., & Anand, R. (2019). Production of biofuel from biomass downdraft gasification and its applications. In A. K. Azad, & M. Rasul (Eds.), *Advanced Biofuels.Applications, Technologies and Environmental Sustainability* (pp. 129-159). Woodhead Publishing. doi:https://doi.org/10.1016/B978-0-08-102791-2.00005-2
32. Kumar, R., Chandrashekar, N., & Pandey, K. K. (2009). Fuel properties and combustion characteristics of Lantana camara and Eupatorium spp. *Current science, 97*(6), 930-934.
33. Lan, W., Ding, H., Jin, X., Yin, D., Wang, Y., & Ji, J. (2022). Catalytic biomass gasification of sawdust:integrated experiment investigation with process modeling and analysis. *International Journal of Low-Carbon Technologies, 17*, 482–487. doi:https://doi.org/10.1093/ijlct/ctac022
34. Lestinsky, P., & Palit, A. (2016). Wood pyrolysis using aspen plus simulation and industrially applicable model . *GeoScience Engineering , 62*(1), 11-16.
35. Li, H., Mou , H., Zhao, N., Yu , Y., Hong , Q., Philbert , M., Zhou, Y., Dizaji, H. B., Dong , R. (2021). Nitrogen Migration during Pyrolysis of Raw and Acid Leached Maize Straw. *Sustainability, 13*(7), 3786. doi:https://doi.org/10.3390/su13073786

36. Li, H., Yu, Y., Yi, F., Qiang, J., Li, C., Zhao, N., Dong, R. (2022). Characteristics and formation of nitrogen-containing products from the pyrolysis of maple wood and maize straw. *Journal of Analytical and Applied Pyrolysis, 163,* 105462. doi:https://doi.org/10.1016/j.jaap.2022.105462
37. Li, L., Liu, G., Li, Y., Zhu, Z., Xu, H., Chen, J., & Ren, X. (2020). Release of Sulfur and Nitrogen during Co-pyrolysis of Coal and Biomass under Inert Atmosphere. *ACS Omega, 5*(46), 30001–30010. doi:https://doi.org/10.1021/acsomega.0c04372
38. Li, X., Wei, Y., Xu, J., Xu, N., & He, Y. (2018). Quantitative visualization of lignocellulose components in transverse sections of moso bamboo based on FTIR macro- and micro-spectroscopy coupled with chemometrics. *Biotechnology for biofuels, 11(1),* 1-16. doi: 10.1186/s13068-018-1251-4
39. López , N. G. (2016). *Biomass utilization for energy purposes in Kenya.* Retrieved 25 January, 2021, from https://www.diva-portal.org/smash/get/diva2:1037533/FULLTEXT01.pdf
40. Lv, D., Xu, M., Liu, X., Zhan, Z., Li, Z., & Yao, H. (2010). Effect of cellulose, lignin, alkali and alkaline earth metallic species on biomass pyrolysis and gasification. *Fuel processing Technology, 91*, 903-909. doi:10.1016/j.fuproc.2009.09.014
41. Meng, X., Rokni, E., Zhou, W., Qi, H., Sun, R., & Levendis, Y. A. (2020). Emissions From Oxy-Combustion of Raw and Torrefied Biomass. *Journal of Energy Resources Technology, 142(12),* 122307-122316 . https://doi.org/10.1115/1.4047330
42. Mierzwa-Hersztek, M., Gondek, K., Jewiarz, M., & Dziedzic, K. (2019). Assessment of energy parameters of biomass and biochars, leachability of heavy metals and phytotoxicity of their ashes. *21*, 786-800. https://doi.org/10.1007/s10163-019-00832-6
43. Ministry of energy and mineral development. (2015). *Uganda's sustainable energy for all (SE4AII) initative action agenda.* Ministry of energy and mineral development , Kampala:. Retrieved 5 November, 2020, from https://www.seforall.org/sites/default/files/Uganda_AA_EN_Released.pdf
44. Mohan, D., Pittman, C. U., & Steele, P. H. (2006). Pyrolysis of wood/biomass for bio-oil: A critical review. *Energy and fuels, 20*, 848-889. doi:10.1021/ef0502397
45. Mundike, J., Collard, F.-X., & Görgens, J. F. (2017). Pyrolysis of Lantana camara and Mimosa pigra: Influences of temperature,other process parameters and incondensable gas evolution on char yield and higher heating value. *Bioresource Technology, 243*, 284-293. doi:10.1016/j.biortech.2017.06.086
46. Nandiyanto, A. B., Oktiani, R., & Ragadhita , R. (2019). How to Read and Interpret FTIR Spectroscope of Organic Material. *Indonesian Journal of Science & Technology, 4*(1), 97-118. doi: http://dx.doi.org/10.17509/ijost.v4i1.15806
47. Neves, D., Thunman, H., Matos, A., Tarelho, L., & Gómez-Barea, A. (2011). Characterization and prediction of biomass pyrolysis products. *Progress in Energy and Combustion Science, 37*(5), 611-630. doi:https://doi.org/10.1016/j.pecs.2011.01.001
48. Nunes, L., De Oliveira Matias, J., & Da Silva Catalao, J. (2018). *Introduction, Torrefaction of biomass for energy applications.* Academic Press, pp 1– 43. doi:10.1016/b978-0-12-809462-4.00001-8
49. Okalebo, R. J., Gathua, K. W., & Woomer, P. L. (2002). *Laboratory methods of soil and plant analysis: A wroking manual* (Vol. 2). TSBF-CIAT and SACRED Africa, Nairobi, Kenya.
50. Osman, A. I., Mehta, N., Elgarahy, A. M., Al-Hinai, A., Al-Muhtaseb, A. H., & Rooney , D. W. (2021). Conversion of biomass to biofuels and life cycle assessment: a review. *Environmental Chemistry Letters, 19*, 4075–4118. doi:https://doi.org/10.1007/s10311-021-01273-0
51. Patel, B., & Gami, B. (2012). Biomass characterization and its use as a solid fuel for combustion. *Iranica Journal of energy and environment, 3*(2), 123-128. doi:10.5829/idosi.ijee.2012.03.02.0071
52. Peters, J. F., Banks, S. W., Bridgwater, A. V., & Dufour, J. (2017). A kinetic reaction model for biomass pyrolysis processes in Aspen Plus. *Applied Energy, 188*, 595-603. doi:https://doi.org/10.1016/j.apenergy.2016.12.030
53. Rocha, S., Candia, O., Valdebenito, F., Espinoza-Monje, F. J., & Azocar, L. (n.d.). Biomass quality index:Searching for suitable biomass as an energy source in Chile. *Fuel*, *264*, 116820. doi:https://doi.org/10.1016/j.fuel.2019.116820
54. Rokni, E., Ren, X., Panahi, A., & Levendis, Y. A. (2018). Emissions of SO2, NOx, CO2, and HCl from Co-firing of coals with raw and torrefied biomass fuels. *Fuel, 211*, 363-374. doi:https://doi.org/10.1016/j.fuel.2017.09.049
55. Shahbaz, M., AlNouss, A., Parthasarathy, P., Abdelaal,, A. H., Mackey, H., McKay, G., & Al-Ansari, T. (2022). Investigation of biomass components on the slow pyrolysis products yield using Aspen Plus for

techno-economic analysis. *Biomass Conversion and Biorefinery, 12*, 669-681. doi:https://doi.org/10.1007/s13399-020-01040-1
56. Shao, L.M., Zhang, H., Yao, Q.S., & He, P.J. (2013). SO_2 and NOx emissions from sludge combustion in a CO_2/O_2 atmosphere. *Fuel, 109*, 178-183. doi:https://doi.org/10.1016/j.fuel.2013.01.027
57. Singh, Y. D., Mahanta, P., & Bora, U. (2017). Comprehensive characterization of lignocellulosic biomass through proximate, ultimate and compositional analysis for bioenergy production. *Renewable energy, 103*, 490-500. doi:http://dx.doi.org/10.1016/j.renene.2016.11.039
58. Tabuti, J. R., Dhillion, S. S., & Lye, K. A. (2003). Firewood use in Bulamogi County, Uganda:species selection,harvesting and consumption patterns. *Biomass and Bioenergy, 25*, 581-596. doi:10.1016/S0961-9534(03)00052-7
59. Tian , T., Li, Q., He, R., Tan, Z., & Zhang , Y. (2017). Effects of biochemical composition on hydrogen production by biomass gasification. *International journal of hydrogen energy*, 1-10. doi:http://dx.doi.org/10.1016/j.ijhydene.2017.06.174
60. Tomczyk, A., Sokołowska , Z., & Boguta , P. (2020). Biochar physicochemical properties: pyrolysis temperature and feedstock kind effects. *Reviews in Environmental Science and Bio/Technology, 19*, 191-215. doi:https://doi.org/10.1007/s11157-020-09523-3
61. Tripathi, M., Sahu, J., & Ganesan, P. (2016). Effect of process parameters on production of biochar from biomass waste through pyrolysis: A review. *Renewable and sustainablle energy reviews, 55*, 467-481. doi:http://dx.doi.org/10.1016/j.rser.2015.10.122
62. Tsuchiya, Y., Shimogaki , H., Abe, H., & Kagawa, A. (2010). Inorganic elements in typical Japanese trees for woody biomass fuel. *The Japan Wood Research Society, 56*, 53-63. doi: 10.1007/s10086-009-1055-z
63. Tursi, A. (2019). A review on biomass:Importance, chemistry,classification, and conversion. *Biofuel Research Journal, 22*, 962-979. doi:10.18331/BRJ2019.6.2.3
64. UBOS. (2014, May). Uganda National Household survey 2012/2013. UBOS, Kampala.
65. Van , S., & Robertson , J. (1985). *Analysis of forages and fibrous foods.* Cornell University, Ithaca, N.Y.
66. Wang, J., Minami, E., Asmadi, M., & Kawamoto, H. (2021). Thermal degradation of hemicellulose and cellulose in ball-milled cedar and beech wood. *Journal of wood science, 67(32),*1-14. doi:https://doi.org/10.1186/s10086-021-01962-y
67. Wang, L., Karimi, N., Sutardi, T., & Pau, M. C. (2019). Combustion Characteristics and Pollutant Emissions in Transient Oxy-Combustion of a Single Biomass Particle: A Numerical Study. *Energy and fuels, 33*, 1556-1569. doi: 10.1021/acs.energyfuels.8b03602
68. Williams, L. C., Emerson, R. M., & Tumuluru, J. S. (2017). Biomass Compositional Analysis for Conversion to Renewable Fuels and Chemicals. In J. S. Tumuluru, *Biomass Volume Estimation and Valorization for Energy* (pp. 251-270). IntechOpen. doi: 10.5772/65777
69. Wongsiriamnuay, T., & Tippayawong, N. (2010). Non-isothermal pyrolysis characteristics of giant sensitive plants using thermogravimetric analysis. *Bioresource Technology, 101*, 5638–5644. doi:10.1016/j.biortech.2010.02.037
70. Xu, F., Yu, J., Tesso, T., Dowell , F., & Wang, D. (2013). Qualitative and quantitative analysis of lignocellulosic biomass using infrared techniques: A mini-review. *Applied Energy, 104*, 801-809. doi:10.1016/j.apenergy.2012.12.019
71. Yang, H., Liu, M., Chen, Y., Xin, S., Zhang, X., Wang, X., & Chen, H. (2020). Vapor–solid interaction among cellulose, hemicellulose and lignin. *Fuel, 263,* 116681. doi:https://doi.org/10.1016/j.fuel.2019.
72. Yguatyara de Luna, M., Rodrigues, P. M., Torres, G. A., Eufrázio, d. A., Queiroz, M. J., Elaine, M. S., & Alexsandra de Sousa, R. M. (2019). A thermogravimetric analysis of biomass wastes from the northeast region of Brazil as fuels for energy recovery. *Energy Sources, Part A: Recovery,Utilization, and environmental effects, 41*(13), 1557-1572. doi: 10.1080/15567036.2018.1549132
73. Yu, S., Park, J., Kim, M., Ryu, C., & Park, J. (2019). Characterization of biochar and byproducts from slow pyrolysis of hinoki cypress. *Bioresource Technology Reports, 6*, 217-222. doi:https://doi.org/10.1016/j.biteb.2019.03.009